PCCP

Accepted Manuscript

ROYAL SOCIETY OF CHEMISTRY

www.rsc.org/pccp

PCCP

PAPER

Self-discharge of electrochemical capacitors based on soluble or grafted quinone†

cReceived 00th January 20xx,
Accepted 00th January 20xx

DOI: 10.1039/x0xx00000x

www.rsc.org/

G. Shul and D. Bélanger*

The self-discharge of hybrid electrochemical capacitors based on the redox activity of electrolyte additive or grafted species to the electrode material is investigated simultaneously for the cell and each individual electrode. Electrochemical capacitor using a redox-active electrolyte consisting in hydroquinone added to the electrolyte solution and a redox-active electrode based on anthraquinone-grafted carbon as negative electrode are investigated. The results are analyzed by using Conway kinetic models and compared to those of a common electrochemical double layer capacitor. The self-discharge investigation is complemented by charge/discharge cycling and it is shown that processes affecting galvanostatic charge/discharge cycling and self-discharge rate occurring at each electrode of an electrochemical capacitor are different but related to each other. The electrochemical capacitor containing hydroquinone in the electrolyte exhibits a much quicker self-discharge rate than that using a negative electrode based on grafted anthraquinone with a 50% decay of the cell voltage of the fully charged device in 0.6 and 6 h, respectively. The fast self-discharge of the former is due to the diffusion of benzoquinone molecules (formed at the positive electrode during charging) to the negative electrode, where they are reduced, causing a quick depolarization. The grafting of anthraquinone molecules on the carbon material of the negative electrode led to a much slower self-discharge, which nonetheless occured, by reaction of the reduced form of the grafted species with electrolyte species.

1. Introduction

Electrochemical capacitors based on carbon electrode as active electrode materials have recently attracted significant interest because they can offer energy storage and energy delivery that are characterized by fast discharge time in the order of the seconds.[1,2] Carbon/carbon-based electrochemical capacitors are the most developed devices due to their large capacitance as a result of a high surface area and porosity, good electronic conductivity, availability and relatively low cost.[3,4] Recent studies focused on the development of novel carbon materials, electrolyte and additives in order to improve the energy and power characteristics.[5–7] The working principle of an electrochemical capacitor involves one or both of the following charge storage processes: (i) electrostatic interaction between the charged electrode and ions of electrolyte in both negative and positive electrodes and (ii) electron transfer due to faradaic processes.[2] The faradaic charge transfer occurring at the electrode surface can originate from the redox-active electrode material such as metal oxides/hydroxides,[8,9] electroactive polymers[10] or functionalized carbon electrode[11] as well as from the electrolyte containing redox-active species, such as ferrocene derivatives,[12] halide ions,[13,14] vanadium complexes,[15,16] viologens[17] and quinones.[18–20] The faradaic processes occurring at the electrode surface generally increase the charge storage capacity of an electrochemical capacitor. For example, the iodine/iodide redox reaction on positive carbon-based electrode gives a specific capacitance value of 476 F g^{-1}, however the capacitance of a cell using this positive electrode is equal 75 F g^{-1}, due to limitation of the negative electrode.[14] Moreover, the use of organic redox-active molecules, such as hydroquinone, enables to increase the specific capacitance to value as high as 900 F g^{-1} for the individual electrode[18] or 220 F g^{-1} for the cell.[21] On the other hand, chemisorption of organic redox-active molecules, such as quinones, on the electrode surface significantly increased the specific capacitance in comparison to a pristine electrode.[22] It should be noted here that although the electrochemical performance of quinone-based system has been previously expressed in specific capacitance (e.g. F g^{-1}), it would be more appropriate to use specific charge units (e.g. C g^{-1} or mAh g^{-1}).[22]

Behind the enhanced performance of redox-active electrolyte based electrochemical capacitors, their practical application could suffer from self-discharge, which is the spontaneous voltage decline of the electrochemical capacitor in the charged state.[23] Despite the fact that the self-discharge of electrochemical double layer capacitors has been substantially investigated,[23–26] studies for redox-active electrolyte based electrochemical capacitor are limited.[17,27–29] It has been

Département Chimie, Université du Québec à Montréal, CP8888, Succursale Centre-Ville, Montréal, Québec, Canada H3C 3P8
E-mail : belanger.daniel@uqam.ca
† Electronic Supplementary Information (ESI) available.
See DOI: 10.1039/x0xx00000x

proposed that the migration/diffusion of an active electrolyte between two electrodes is the primary reason of the fast self-discharge process.[27] The introduction of an ion-exchange membrane as separator causes a partial decrease of the self-discharge rate but that is still higher than the self-discharge rate of a conventional electrochemical capacitor without redox-active species in the electrolyte.[27] Furthermore, redox active viologens that can spontaneously adsorb on the charged electrode led to improved performance of the electrochemical capacitor in comparison to electroactive molecules that do not adsorb and also significantly slowed down the self-discharge rate of a redox-active based electrochemical capacitor.

Herein, we describe an approach to further mitigate self-discharge by chemical grafting of anthraquinone molecules to the surface of a carbon black based negative electrode. The self-discharge of the electrochemical capacitor using this electrode is compared with a device using redox-active hydroquinone in the electrolyte. In our study, the cell voltage and the potential variation of negative and positive electrodes was monitored with a reference electrode during both constant current charge/discharge and self-discharge. It was found that the self-discharge of the electrochemical capacitor based on the chemically grafted redox molecules is significantly slower than that making use of a redox active quinone in the electrolyte.

2. Experimental

2.1 Chemicals and materials

Black Pearls 2000 powder (BP) (Cabot Corporation), acetylene black carbon (50% compressed, Alfa Aesar, 99.9+%), graphite powder (Timcal Timrex), poly(tetrafluoroethylene) beads (PTFE) (Aldrich), glassy carbon disk electrode (SPI Supplies/Structure Probe, Inc), 2-aminoanthraquinone (AQ) (Aldrich, tech. grade), tert-butylnitrite (Aldrich, 90%), hydroquinone (HQ) (Alfa Aesar, a.c.s. reagent), sulfuric acid (Fisherbrand, 97%) were used as received. Glass microfiber binder free filter (GF/C grade, pore size 0.7 µm) was purchased from Whatman.

2.2 BP modification and composite electrode preparation

AQ-modified BP (BP-AQ) powder was prepared as reported previously.[30] The estimated value of AQ loading is 15 wt% (average value for five experiments), whereas the total specific capacitance and specific capacity for such electrodes are equal to 151 F g^{-1} and 42 mAh g^{-1} (estimated at 2 mV s^{-1}), respectively. These values are in the range previously reported for BP-AQ electrode.[11] The working electrode consists of a composite film prepared by mixing, in a small volume of ethanol, the modified or unmodified BP powder, acetylene black, graphite and PTFE as binder in an 80:7.5:7.5:5 wt% ratio until a homogenized paste-like consistency was obtained. The paste was cold rolled to the thickness of around 16 µm and dried under vacuum overnight at 70°C. From the resulting film, two 3 mm diameter circles were cut out and placed in a T-shaped tube between two glassy carbon electrodes (current collector) and separated by a glass microfiber filter (separator and electrolyte container) (Scheme SI1). An Ag/AgCl/3MKCl as reference electrode was installed in the third leg of a T-shaped tube. For the experiments performed in a conventional electrochemical cell, the working electrode was prepared by pressing a small square of a carbon film, approximately 0.25 cm^2 and 2 mg in weight, on a stainless steel grid (80 mesh, 0.127 mm, Alfa Aesar) for 60 s at 9×10^5 Pa.

2.3 Electrochemical experiments

The cyclic voltammetry measurements (at a scan rate of 2 mV s^{-1}) were carried out using a potentiostat electrochemical interface SI480 (Solartron Intstruments) linked with a PC and the electrochemical setups were controlled with the DC Corrware software (Scribner associates, version 2.8d). Galvanostatic charge/discharge (GCD) cycling and open-circuit measurements were performed with a VMP3 potentiostat. Prior to any measurements, the BP-based electrodes were kept in the electrolyte for 1 hour in order to allow the electrolyte to impregnate the electrode porosity. The open-circuit potential was recorded after a 1 hour hold time at 1.0 V for BP/BP and BP/BP-AQ cells in 1 M H_2SO_4, and 10 min at 0.8 V for BP/BP in 0.38 M HQ/1 M H_2SO_4. The electrochemical experiments were repeated until the carbon electrodes show steady-state responses (~3-5 self-discharge measurements). The current densities are presented per the total mass of both electrodes.

2.4 Charge balancing

Because it was earlier reported that AQ-functionalized electrode exhibits an enhancement of the charge storage properties compared to unmodified carbon electrode,[11,31] in order to counterbalanced the charge on the opposite electrode, the mass of this latter electrode should be increased accordingly. In practice, the mass of the positive electrode was increased by a factor of 10 in order to clearly distinguish processes occurring at each individual electrode. The details will be discussed below.

3. Results and discussion

In this paper, we are investigating the effect of chemically grafted redox-active molecules on the carbon material of the negative electrode on its self-discharge and that of the full device. The self-discharge is compared with that of a symmetric electrochemical capacitor using or not redox additive quinone species in the electrolyte. The self-discharge mechanism was studied by using Conway kinetic models, which yield the predicted self-discharge time profiles for activation-controlled or diffusion-controlled faradaic processes, or as a cause of ohmic leakage due to a fault in a device construction.[23] The two first models include the electrolyte decomposition as a result of the overcharging beyond the respective decomposition potential limit and the redox reactions due to oxidizable or reducible impurities present in the electrolyte or the electrode material. The charge

redistribution in the pores of the electrode material is also a possible mechanism of the self-discharge process.[24,26,32] These studies are complemented by initial constant current charge/discharge experiments of the three different electrochemical capacitors.

3.1 Constant current charge/discharge

Fig. 1 (a) shows the typical rectangular shape cyclic voltammogram recorded for a symmetric carbon/carbon electrochemical capacitor with 1 M H_2SO_4 as electrolyte. The oxidation wave at 0.06 V is associated to the quinone groups generated during potential cycling.[33] The galvanostatic charge/discharge profile of the cell is nearly triangular with a Coulombic efficiency of over 97% (Fig. 1, b). Also, the shape of the galvanostatic charge/discharge profile for each individual electrode is almost triangular (Fig. 1, c), with the appearance of a sloped plateau at higher potential for the positive electrode. This is probably due to the electrolyte decomposition,[34] which is causing a non symmetrical variation of the potential of the positive and negative electrodes (Fig. 1, c). Nonetheless, the overall potential profiles are characteristic of an electrostatic charge storage mechanism that is typical for a symmetric electrochemical double-layer capacitor.[4,35]

In the presence of hydroquinone as a redox additive in the electrolyte, the shape of the cyclic voltammogram and charge/discharge profiles change noticeably (Fig. 2). The redox wave with a peak at 0.03 V is clearly visible on the cyclic voltammogram (Fig. 2, a), as previously observed for activated carbon electrodes,[18,20] while it was not detectable for the graphene hydrogel material.[27] The faradaic reaction of the hydroquinone/benzoquinone system contributes to the charge storage processes.[20,21] The faradaic contribution is also observable on the charge/discharge profile of the full cell (Fig. 2, b) that deviates from the triangular shape, most obviously, in the low voltage region. The lower operating voltage of the cell is caused by the shift of the potential range of the negative and positive electrodes that are not already symmetrical as in the BP/BP system. The potential of the positive electrode, where the faradaic process of benzoquinone/hydroquinone conversion (Eq. 1) takes place, remains almost independent of the state of charge during the charge/discharge process.[20,21,27,35]

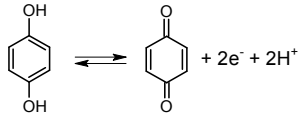

(1)

This electrode behaves as a non-polarizable electrode and operates in a very narrow potential range (20 mV) close to the equilibrium potential of 0.40 V vs. Ag/AgCl (Fig. 2, c). The redox potential roughly estimated for reaction (1) (SI, section 2) and obtained from the cyclic voltammogram for a BP electrode in 0.38 M HQ/1 M H_2SO_4 in the three-electrode configuration (Fig. SI1, a) is 0.35 and 0.45 V vs. Ag/AgCl, respectively, in agreement with previous studies (0 V vs. Hg/Hg_2SO_4).[21] On the other hand, the negative electrode operates over a wider potential range (780 mV), which almost exclusively contributes to the voltage of the cell (Fig. 2, c).

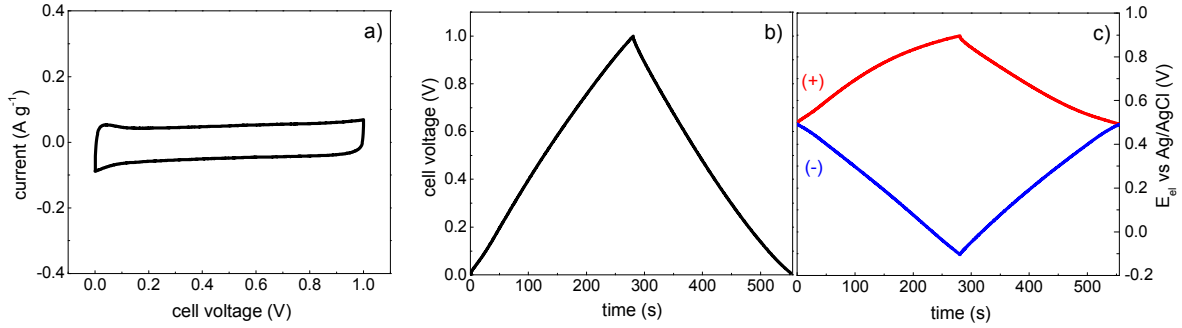

Fig.1 Cyclic voltammogram (a), galvanostatic charge/discharge profiles for the cell (b, left axis) and separately for positive and negative electrodes (c, right axis) of an electrochemical capacitor composed of BP/BP electrodes (mass ratio is 1:1) in 1M H_2SO_4 electrolyte. Current density is 90 mA g^{-1}.

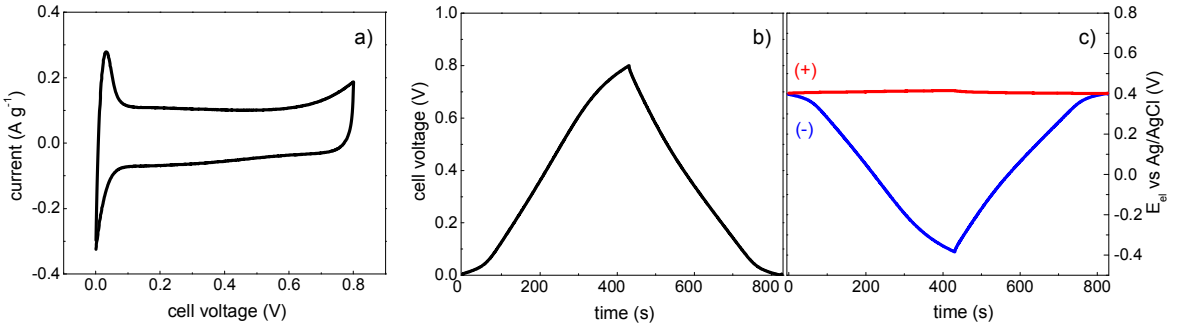

Fig. 2 Cyclic voltammogram (a), galvanostatic charge/discharge profiles for the cell (b, left axis) and separately for positive and negative electrodes (c, right axis) of an electrochemical capacitor composed of BP/BP electrodes (mass ratio is 1:1) in 0.38 M HQ in 1M H_2SO_4 electrolyte. Current density is 90 mA g^{-1}.

PCCP

PAPER

A sloped plateau observed at the beginning of charging at 0.4 V vs. Ag/AgCl for the negative electrode (Fig. 2, c) is due to the reduction of benzoquinone molecules that diffuse from the positive to the negative electrode. In addition, the potential of the negative electrode during the charge process reaches a value of -0.4 V that is more negative than the thermodynamic potential needed for hydrogen evolution in the presence of the aqueous acid electrolyte used in this work.[36] This explains both the deviation of the shape of the galvanostatic charge/discharge curves from a triangular shape (Coulombic efficiency is 92%) (Fig. 2, c) and the increase of the current at 0.8 V on the cyclic voltammogram of the cell (Fig. 2, a).

The mechanism of the charge storage in an electrochemical capacitor containing a redox additive electrolyte has been recently discussed.[37] It was proposed that in order to participate in the charge storage process, the redox species need to enter the pores of the electrode, where they undergo redox interconversion on the internal and external surfaces of the electrode that is directly responsible for the enhancement of the charge storage capacity. If the products of the oxidation are soluble, they can diffuse through the pores and enter the bulk electrolyte causing irreversibility and self-discharge if they are eventually being converted back to the initial form of the redox couple at the positive electrode.[37]

In order to avoid possible migration and diffusion of redox products in the electrolyte, redox active anthraquinone molecules were chemically attached to the BP porous carbon. For this purpose, AQ-modified BP (BP-AQ) powder was used to fabricate the negative electrode. Fig. 3 shows the cyclic voltammogram and galvanostatic charge/discharge profiles recorded for the asymmetric BP/BP-AQ electrochemical capacitor.

The cyclic voltammogram of a two-electrode cell exhibits a capacitive region between 0 and 0.7 V that is followed by an apparent reversible redox system centred at 0.89 V (Fig. 3, a) associated with the electrochemical conversion of AQ molecules into dihydroxyanthracene (AQH_2) grafted on the BP surface (Eq. 2).

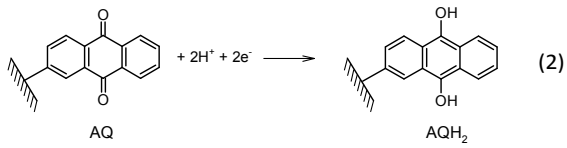

(2)

The galvanostatic charge/discharge profile recorded for the cell shows two linear regions of different slopes also indicating different nature of the charge storage process. The Coulombic efficiency of this device is 95%, similar to that observed for BP/BP in 1 M H_2SO_4. During cycling, the potential of the positive electrode varies linearly between 0.5 and 0.7 V (Fig. 3, c) as expected from the cyclic voltammogram of a BP electrode recorded in the three-electrode configuration (Fig. SI1, b). For the negative electrode, the potential variation between 0.5 and 0 V arises from the charge storage contribution of BP, whereas the sloped plateau between 0 and -0.2 V is due to the interconversion of the grafted anthraquinone[11] that is clearly demonstrated by the cyclic voltammogram obtained for BP-AQ film as working electrode in the three-electrode configuration (Fig. SI1, b). Below a potential of -0.2 V, the slope of the potential dependence for the negative electrode is changing again, probably due to solvent decomposition after the complete reduction of the grafted anthraquinone (Eq. 2). In contrast to the device containing soluble HQ redox species, the BP/BP-AQ electrochemical capacitor contains almost a three order of magnitude smaller amount of redox species: ca. 1×10^{-7} and 8×10^{-5} mol for the electrochemical capacitors containing AQ and HQ, respectively.

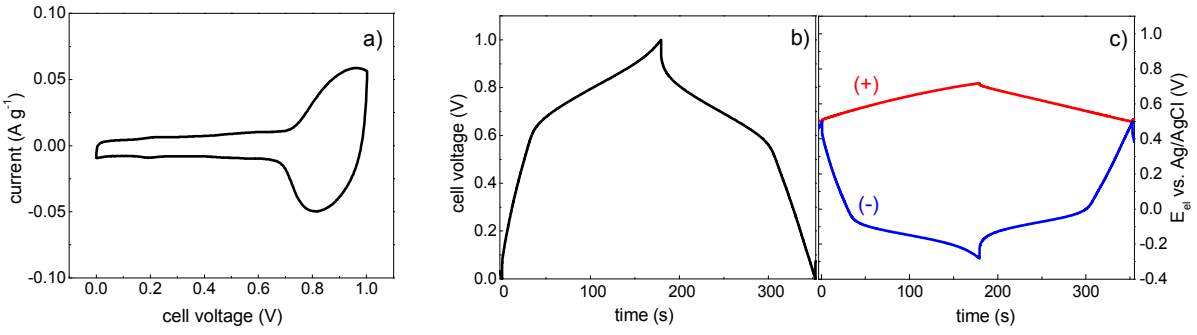

Fig. 3 Cyclic voltammogram (a), galvanostatic charge/discharge profiles for the cell (b, left axis) and separately for positive and negative electrodes (c, right axis) of an electrochemical capacitor composed of BP/BP-AQ electrodes (mass ratio is 10:1) in 1M H_2SO_4 electrolyte. Current density is 50 mA g^{-1}.

PCCP

PAPER

Nonetheless, if the faradaic charge is normalized for the number of moles of quinone per mass of negative and positive electrodes for the electrochemical capacitor containing AQ and HQ, respectively, specific charge of 4.6×10^8 and 2.9×10^5 C g^{-1} mol^{-1} (SI, section 3) are obtained. This is a three-order of magnitude higher quinone utilization for the AQ grafted carbon electrode than for the carbon electrode with soluble HQ.

In addition, it can be observed that when an electrochemical capacitor with electrodes having a BP/BP-AQ mass ratio of 10:1 is being charged, the negative electrode operates over the whole range of AQ electroactivity (between 0 and -0.3 V vs. Ag/AgCl). Whereas for the BP/BP-AQ cell with a mass ratio of 5:1 (Fig. SI2) and 1:1 (Fig. SI3), the potential of the negative electrode just reaches the reduction peak (-0.2 V vs. Ag/AgCl) or does not even approach it (0 V vs. Ag/AgCl), respectively. It can be concluded that, as expected, in order to benefit from the charge storage of the grafted AQ molecules, their voltammetric charge should be entirely counterbalanced by using an appropriate mass of BP for the positive electrode. Similar correlation between charge and mass for hybrid electrochemical capacitors based on conducting polymers has been previously done.[38] Obviously, using a 10:1 mass ratio for the positive and negative electrodes could not be practical and a real device would require a positive electrode with a higher charge storage capacity. This could be obtained by grafting suitable redox species on the positive electrode.[39,40]

3.2 Self-discharge

Fig. 4 shows self-discharge profiles recorded for a BP/BP electric double layer capacitor in 1 M H_2SO_4 as electrolyte. The cell voltage declines from 1 to about 0.5 V during the first 10000 s (Fig. 4, a). This potential decrease is smaller than that observed for electrochemical capacitor fabricated with electrode based on graphene hydrogel.[27] Interestingly, it can be observed that despite the symmetry of the BP/BP cell, the self-discharge rate of the negative electrode is slightly higher than that for the positive electrode (Fig. 4, a), suggesting different self-discharge processes for two electrodes. For this symmetric device, the potential shift from the equilibrium potential is about 0.5 V for each individual electrode upon charging (Fig. 1, c), thus the driving force for self-discharge due to potential field[41] is assumed to be equal for both electrodes. The self-discharge mechanism of the positive and negative electrodes were investigated by fitting the potential-time curves according to Conway models[23] (Figs. 4, b and c). While the positive electrode does not show a linear dependence neither versus log time nor time$^{1/2}$ (Figs. 4, b and c, red lines) the negative electrode clearly exhibits a lack of linearity of E_{el} vs. time$^{1/2}$ (Fig. 4, c) and a linear relationship between E_{el} and log time after an initial plateau (Fig. 4, b). The latter is consistent with an activation-controlled self-discharge mechanism, which is probably associated to the oxygen reduction process on naturally present quinone groups on the carbon surface.[42] Because of the cell construction, it was impossible to purge the electrolyte with nitrogen gas. An irreversible reduction peak was clearly observed at 0.01 V for unmodified BP electrode in O_2 saturated solution (Fig. SI4, a). The impact of oxygen reduction on the negative electrode has been studied earlier in a conventional three-electrode electrochemical cell and the self-discharge process was found to be diffusion-controlled.[43]

In the case of the electrochemical capacitor with the redox active electrolyte (0.38 M HQ in 1 M H_2SO_4), the cell is fully self-discharged to 0 V in less than 13000 s (Fig. 5).

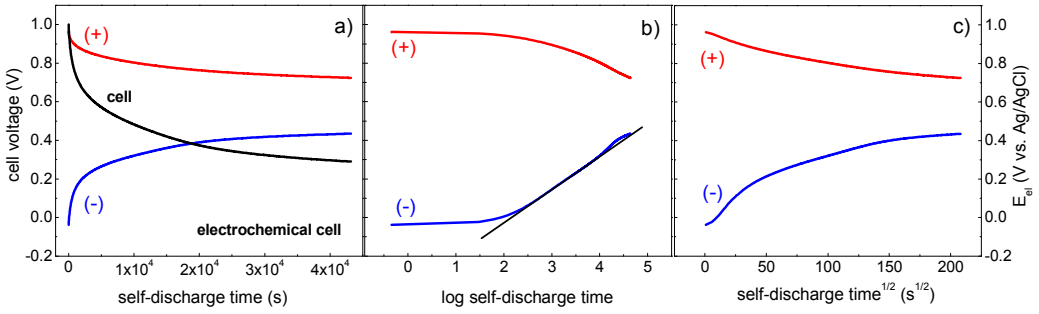

Fig.4 Self-discharge profiles of an electrochemical capacitor composed of BP/BP films (mass ratio 1:1) with 1 M H_2SO_4 for cell (black line) with potential changes of the positive electrode (red) and the negative electrode (blue) plotted as function of (a) self-discharge time, (b) log self-discharge time; and (c) self-discharge time$^{1/2}$.

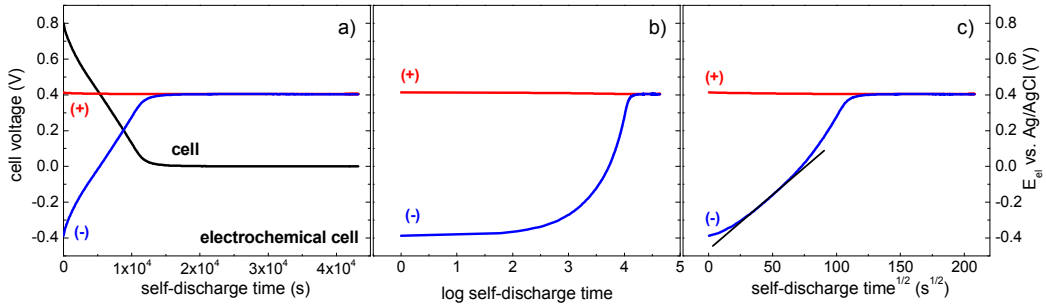

Fig. 5 Self-discharge profiles of an electrochemical capacitor composed of BP/BP films (mass ratio 1:1) with 0.38 M HQ in 1 M H_2SO_4 for cell (black line) with potential changes of the positive electrode (red) and the negative electrode (blue) plotted as function of (a) self-discharge time, (b) log self-discharge time; and (c) self-discharge time$^{1/2}$.

The self-discharge voltage profiles recorded for both electrodes differ significantly, as expected from galvanostatic charge/discharge measurements (Fig. 2). While the potential of the positive electrode remains close to its equilibrium potential, the overall self-discharge is almost completely caused by the negative electrode (Fig. 5). Three factors can have an influence on the self-discharge process: (i) the thermodynamic effect – the potential of the negative electrode in the fully charged state is much more further from the equilibrium potential than that of the positive electrode; (ii) the shuttle effect – benzoquinone molecules generated at the positive electrode during charging can diffuse to the negative electrode, where they are reduced (Scheme 1, a),[27] and (iii) the hydrogen evolution reaction. Only the negative electrode can possibly be affected by these factors, thus causing high asymmetry in self-discharge rates of the two electrodes. A lack of linearity is observed in the E_{el} vs. log time plot (Fig. 5, b), while the E_{el} vs. time$^{1/2}$ dependence is linear during a fraction of the discharge time (Fig. 5, c).[23] Such behaviour indicates the impact of benzoquinone diffusion on the self-discharge process (SI, section 6).

On the other hand, the shuttle effect can be presumably excluded for a hybrid electrochemical capacitor with redox compound chemically bonded to the carbon surface, as it is the case for AQ-modified BP electrode. The self-discharge is clearly much slower than that observed with the redox-active electrolyte and the self-discharge profile shows three distinct regions. The initial voltage drop (first 1000 s) (Fig. 6, a, black line) is most probably due to electrolyte decomposition that is observed on galvanostatic charge/discharge curves (Fig. 3, c). Then, the rate of self-discharge slows down until the noticeable inflection point at 20000 s that is followed by a faster voltage decline down to 0.1 V (Fig. 6, a, black line). From the potential profiles recorded for individual electrodes, it can be observed that the self-discharge of the full cell between 0.8 and 0.7 V is mainly due to the self-discharge of the grafted redox species (namely, oxidation of AQH_2 (Scheme 1, c)) on the negative electrode (Fig. 6, black and blue lines), which occurs between -0.20 and 0.05 V vs. Ag/AgCl (Fig. SI1, b). Due to the oxidation of AQH_2, the potential of the negative electrode decreases slowly. In the same time region, the linear dependence of E_{el} vs. log time is observable (Fig. 6, b, blue line), indicating an activation-controlled self-discharge process.[23] As soon as the oxidation of AQH_2 grafted molecules is complete (after the first 20000 s) the potential declines at a much higher rate (Fig. 6, a, blue line) and approaches the equilibrium potential that is close to the value observed for the BP/BP system in 1 M H_2SO_4 (Scheme 1, d). Similarly to unmodified BP electrode, we speculate that the oxygen reduction reaction at around 0 V (Fig. SI4, b) has an influence on self-discharge process. Indeed, AQ-modified glassy carbon can act as catalyst for the electrochemical oxygen reduction, however in acid solution the kinetics of this reaction are very sluggish.[44] The positive electrode, similarly to the BP/BP system in 1 M H_2SO_4 (Fig. 4), reveals a slow self-discharge process (Fig 6, red lines). Because of the high mass loading of the BP positive electrode, a small decline (ΔE = 0.06 V) of potential is observed. The linear variation of the E_{el} vs. time$^{1/2}$ plot (Fig. 6, c, red line) might be due to the reduction of the AQ molecules that are not covalently bonded to the BP of the negative electrode and that diffuse to the positive electrode.

Because the reoxidation of AQH_2 takes place during the self-discharge, the electron participating in this reaction can be transferred to the BP carbon support or to solution species (e.g. dissolved oxygen, electrolyte impurities). Obviously, these two processes will give opposite effect on the self-discharge profile. Theoretically, the former should cause the shift of the electrode potential towards negative value or at least a significant slowdown of the rate of self-discharge should be observed due to influence of other process causing the self-discharge, as it happens on the electrode composed of unmodified carbon. Contrary to that, the reoxidation of grafted AQH_2 by species present in a solution will cause self-discharge.

To get a better understanding of this phenomenon, the self-discharge profiles for single BP, BP-AQ and mixture of BP and BP-AQ electrodes and charged to the same potential value were recorded in a conventional electrochemical cell containing a large volume (50 mL) of electrolyte (Fig. 7). The shape of the obtained profiles are similar to those obtained in

the electrochemical capacitor cell configuration (Scheme SI1), where the exponential and double bend curves are observed for BP (Fig. 7, a) and BP-AQ (Figs. 7, b, c) electrodes, respectively.

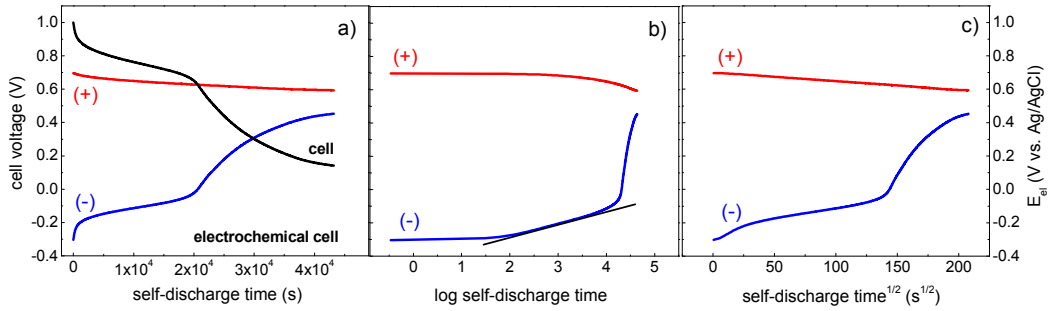

Fig.6 Self-discharge profiles of an electrochemical capacitor composed of BP/AQ-BP films (mass ratio 10:1) with 1 M H_2SO_4 for cell (black line) with potential changes of the positive electrode (red) and the negative electrode (blue) plotted as function of (a) self-discharge time, (b) log self-discharge time; and (c) self-discharge time$^{1/2}$.

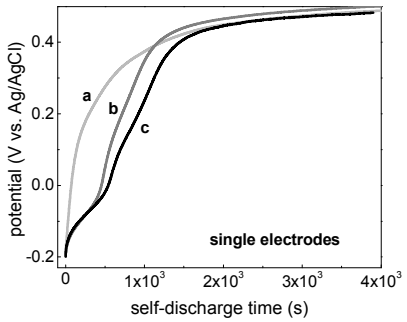

Fig. 7 Self-discharge profiles of a single electrode composed of $BP_{(100\%)}$ (a, light gray line), $BP_{(50\%)}$/$BP\text{-}AQ_{(50\%)}$ (b, gray line) and $BP\text{-}AQ_{(100\%)}$ (c, black line) in 1 M H_2SO_4 after pre-charge at -0.2 V for 1 hour.

However, a difference is noticeable in the timescale needed for the complete self-discharge of the redox molecules of the electrode composed of $BP\text{-}AQ_{(100\%)}$, which lasted for only 500 s (Fig. 7, c) in comparison to 2×10^4 s for the same modified carbon in the electrochemical capacitor (Fig. 6). This large discrepancy can be due to the larger volume of the aqueous solution, namely to the amount of the species present therein. The species, that can oxidize AQH_2 and influence the self-discharge process, are presumably dissolved oxygen molecules,[45] electrolyte impurities such as iron (III) ions[43] or others. In addition, in the case of the electrode containing a smaller amount of the redox molecules ($BP_{(50\%)}$/$BP\text{-}AQ_{(50\%)}$), the self-discharge time is shorter, ca. 420 s (Fig. 7, b). However, as mentioned above, the transfer of electrons to the BP substrate during reoxidation of AQH_2 is not completely excluded.

The phenomena giving rise to the observed self-discharge behaviour are summarized on Scheme 1. The main drawbacks of electrochemical capacitor containing HQ (Scheme 1, a and b) are: (i) the non-polarizability of the positive electrode and as a consequence, a lower cell voltage due to the negative electrode limitation and (ii) the extremely high self-discharge of the cell mainly due to the shuttle effect – the transfer of redox species from the positive to the negative electrode, where they are spontaneously reduced. With the electrochemical capacitor containing only chemically bonded AQ (Scheme 1, c and d), the shuttle effect can be eliminated. The reoxidation of AQH_2 slows down the rate of self-discharge, at least during the time required for the complete electrochemical conversion of AQH_2 that is probably taking place by reaction with oxygen or impurities dissolved in the aqueous solution. Moreover, both electrodes are polarizable and contribute to the cell voltage. Nonetheless, as mentioned above, the charge balancing by varying the mass of the electrodes is a disadvantage of this device. Further experiments along these lines are in progress.

Conclusions

In summary, this paper clearly shows that attaching AQ molecules by a covalent bond with a carbon support can significantly slows down the self-discharge in comparison to the case when electroactive quinone are dissolved in the electrolyte. The self-discharge of three different types of electrochemical capacitors was investigated by simultaneous recording of the positive and negative electrode potentials against a reference electrode. Our data show that processes occurring at each electrode differ during charge/discharge or self-discharge.

PCCP

PAPER

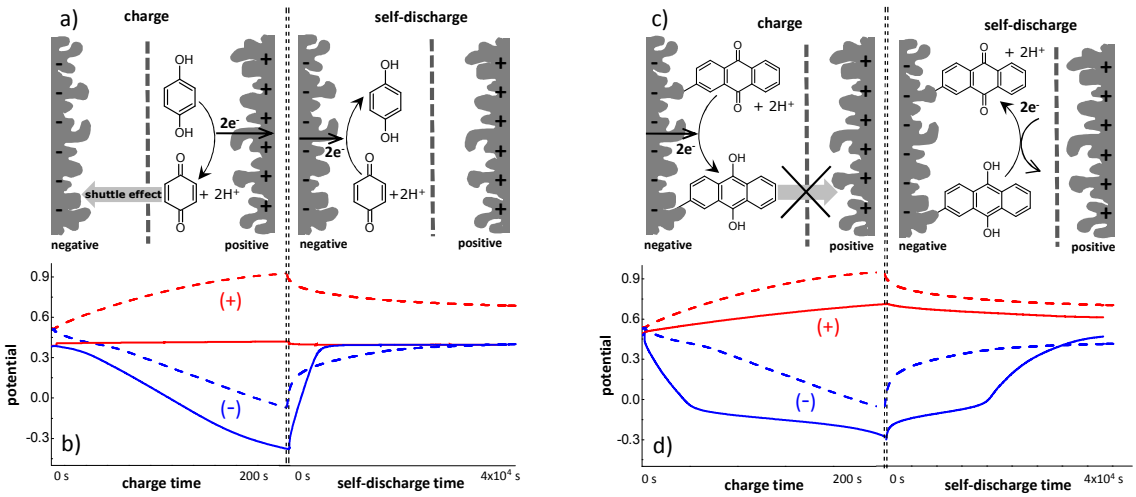

Scheme 1. Schematic drawings of the electrochemical reactions occurring during charge and self-discharge in electrochemical capacitors containing HQ (a) and AQ (c) redox species. Separator is indicated by the grey dashed line. The corresponding potential profiles of individual electrodes for electrochemical capacitors containing HQ (b, solid lines), (AQ) (d, solid lines) and those observed for electrochemical capacitor without redox species (b and d, dashed lines).

Thus, the potential application of HQ as a redox additive into electrolyte in electrochemical capacitor suffers from two main issues: (i) the positive electrode, where HQ oxidation takes place, is hardly polarisable and causes a lower cell voltage due to limitations of the negative electrode; (ii) the depolarization of the negative electrode by the products of electrochemical reaction on the positive electrode, so-called, shuttle effect. Both cause a high-rate of self-discharge of the negative electrode and consequently of the cell. A model describing diffusion-controlled self-discharge mechanism that is considering all dynamic parameters of the system with redox-active electrolyte is not currently available in the literature and must be developed.

A possible mitigation of self-discharge would be possible if the soluble redox species formed upon charging remained adsorbed within the porous carbon structure as is the case for iodide-based redox active electrolyte.[29] In practical application, the self-discharge drawback can be avoided by recharging the redox-active electrochemical capacitor just before use or by application of float charging during extended storage.[46] Furthermore, a recent study, which proposes an intermediate approach between having soluble and grafted electroactive species in an electrochemical capacitor, showed that electroactive viologens having strong adsorption properties can significantly decrease the self-discharge rate.[17] In the case of electrochemical capacitor containing AQ attached to the carbon support for the negative electrode, mitigation of the self-discharge is observed during the timescale where the redox reaction of the reduced grafted quinone molecules with electrolyte species is taking place. Further investigation on the different combinations of materials for the positive and negative electrodes of electrochemical capacitors is required.

Acknowledgements

The financial support of the Natural Science and Engineering Research Council of Canada (NSERC) is gratefully acknowledged.

References

1 L. L. Zhang and X. S. Zhao, *Chem. Soc. Rev.*, 2009, **38**, 2520–2531.
2 B. E. Conway, *Electrochemical Capacitors – Scientific Fundamentals and Technological Applications*, 1999.
3 E. Frackowiak, Q. Abbas and F. Béguin, *J. Energy Chem.*, 2013, **22**, 226–240.
4 E. Frackowiak and F. Béguin, *Carbon N. Y.*, 2001, **39**, 937–950.
5 P. Simon and Y. Gogotsi, *Nat. Mater.*, 2008, **7**, 845–854.
6 Z. Cao and B. B. Q. Wei, *Energy Environ. Sci.*, 2013, **6**, 3183–3201.
7 R. R. Salunkhe, Y.-H. Lee, K.-H. Chang, J.-M. Li, P. Simon, J. Tang, N. L. Torad, C.-C. Hu and Y. Yamauchi, *Chem. - A Eur. J.*, 2014, **20**, 13838–13852.

8 W. Deng, X. Ji, Q. Chen and C. E. Banks, *RSC Adv.*, 2011, **1**, 1171–1178.
9 J. H. Park, O. O. Park, K. H. Shin, C. S. Jin and J. H. Kim, *Electrochem. Solid-State Lett.*, 2002, **5**, H7–H10.
10 L. Nyholm, G. Nyström, A. Mihranyan and M. Strømme, *Adv. Mater.*, 2011, **23**, 3751–3769.
11 G. Pognon, T. Brousse, L. Demarconnay and D. Bélanger, *J. Power Sources*, 2011, **196**, 4117–4122.
12 M. Tachibana, T. Ohishi, Y. Tsukada, A. Kitajima, H. Yamagishi and M. Murakami, *Electrochemistry*, 2011, **79**, 882–886.
13 G. Lota and E. Frackowiak, *Electrochem. Commun.*, 2009, **11**, 87–90.
14 J. Menzel, K. Fic, M. Meller and E. Frackowiak, *J. Appl. Electrochem.*, 2014, **44**, 439–445.
15 E. Frackowiak, K. Fic, M. Meller and G. Lota, *ChemSusChem*, 2012, **5**, 1181–1185.
16 S. T. Senthilkumar, R. K. Selvan and J. S. Melo, *J. Mater. Chem. A*, 2013, **1**, 12386–12394.
17 S.-E. Chun, B. Evanko, X. Wang, D. Vonlanthen, X. Ji, G. D. Stucky and S. W. Boettcher, *Nat. Commun.*, 2015, **6**, 7818.
18 S. Roldán, C. Blanco, M. Granda, R. Menéndez and R. Santamaría, *Angew. Chem. Int. Ed.*, 2011, **50**, 1699–1701.
19 W. Chen, R. B. Rakhi and H. N. Alshareef, *Nanoscale*, 2013, **5**, 4134–4138.
20 E. Frackowiak, M. Meller, J. Menzel, D. Gastol and K. Fic, *Faraday Discuss.*, 2014, **172**, 179–198.
21 S. Roldan, M. Granda, R. Men, R. Santamaría and C. Blanco, *J.Phys.Chem.C*, 2011, **115**, 17606–17611.
22 B. D. Assresahegn, T. Brousse and D. Bélanger, *Carbon N. Y.*, 2015, **92**, 362–381.
23 B. E. Conway, W. G. Pell and T.-C. Liu, *J. Power Sources*, 1997, **65**, 53–59.
24 A. Lewandowski, P. Jakobczyk, M. Galinski and M. Biegun, *Phys. Chem. Chem. Phys.*, 2013, **15**, 8692–8699.
25 H. A. Andreas, *J. Electrochem. Soc.*, 2015, **162**, A5047–A5053.
26 M. Kaus, J. Kowal and D. U. Sauer, *Electrochim. Acta*, 2010, **55**, 7516–7523.
27 L. Chen, H. Bai, Z. Huang and L. Li, *Energy Environ. Sci.*, 2014, **7**, 1750–1759.
28 L. Chen, Y. Chen, J. Wu, J. Wang, H. Bai and L. Li, *J. Mater. Chem. A*, 2014, **2**, 10526–10531.
29 Q. Abbas and F. Béguin, *Prog. Nat. Sci. Mater. Int.*, 2015, **25**, 622–630.
30 G. Pognon, T. Brousse and D. Bélanger, *Carbon N. Y.*, 2011, **49**, 1340–1348.
31 X. Chen, H. Wang, H. Yi, X. Wang, X. Yan and Z. Guo, *J.Phys.Chem.C*, 2014, **118**, 8262–8270.
32 J. Black and H. A. Andreas, *Electrochim. Acta*, 2009, **54**, 3568–3574.
33 J. V. Hallum and H. V Drushel, *J. Phys. Chem.*, 1958, **62**, 110–117.
34 S. Ban, J. Zhang, L. Zhang, K. Tsay, D. Song and X. Zou, *Electrochim. Acta*, 2013, **90**, 542–549.
35 S. Roldán, D. Barreda, M. Granda, R. Menéndez, R. Santamaría and C. Blanco, *Phys. Chem. Chem. Phys.*, 2015, **17**, 1084–1092.
36 M. P. J. Brennan and O. R. Brown, *J. Appl. Electrochem.*, 1972, **2**, 43–49.
37 B. Akinwolemiwa, C. Peng and G. Z. Chen, *J. Electrochem. Soc.*, 2015, **162**, A5054–A5059.
38 D. Villers, D. Jobin, C. Soucy, D. Cossement, R. Chahine, L. Breau and D. Bélanger, *J. Electrochem. Soc.*, 2003, **150**, A747–A752.
39 E. Lebègue, T. Brousse, J. Gaubicher, R. Retoux and C. Cougnon, *J. Mater. Chem. A*, 2014, **2**, 8599–8602.
40 N. An, Y. An, Z. Hu, B. Guo, Y. Yang and Z. Lei, *J. Mater. Chem. A*, 2015, **3**, 22239–22246.
41 Q. Zhang, J. Rong and B. Wei, *RSC Adv.*, 2011, **1**, 989–994.
42 T. Nagaoka, T. Sakai, K. Ogura and T. Yoshino, *Anal. Chem.*, 1986, **58**, 1953–1955.
43 H. A. Andreas, K. Lussier and A. M. Oickle, *J. Power Sources*, 2009, **187**, 275–283.
44 G. Jürmann, D. J. Schiffrin and K. Tammeveski, *Electrochim. Acta*, 2007, **53**, 390–399.
45 A. M. Oickle and H. A. Andreas, *J. Phys. Chem. C*, 2011, **115**, 4283–4288.
46 R. Nozu, M. Iizuka, M. Nakanishi and M. Kotani, *J. Power Sources*, 2009, **186**, 570–579.